SiliconPV 2012, 03-05 April 2012, Leuven, Belgium

Ultrasonic Bonding of Aluminum Ribbons to Interconnect High-Efficiency Crystalline-Silicon Solar Cells

M. Heimann[a]*, P. Klaerner[b], C. Luechinger[b], A. Mette[a], J. W. Mueller[a], M. Traeger[a], T. Barthel[a], O. Valentin[b], P. Wawer[a]

[a]Q-Cells SE, Sonnenallee 17 - 21, 06766 Bitterfeld-Wolfen, Germany
[b] Kulicke and Soffa Industries, Inc., Wedge Bonder Business Unit, 16700 Red Hill Ave, Irvine, CA 92606-4802, USA

Abstract

Next-generation, crystalline-silicon solar cells might use different metallization concepts compared to current state-of-the-art cell designs. One specific design uses a thin aluminum back layer created with a physical vapor deposition process. In the solar industry, there is no reliable, cost-effective method of directly connecting metallic ribbons to such an aluminum layer to create cell strings. In the semiconductor industry ultrasonically bonding aluminum ribbon to the aluminum metallization of power semiconductors or high-volume production is a well-established process. This paper describes adapting ultrasonic ribbon bonding and the equipment used in the semiconductor industry to interconnect crystalline-silicon solar cells.

1. Introduction

Next-generation, high-efficiency, crystalline-silicon (c-Si) solar cells create new requirements for the technologies used to interconnect cells inside a module. Advanced cells have different structures, and in particularly, use different metallization concepts than current state-of-the-art cell designs. Certain designs use an aluminum (Al) back layer that is typically 1µm to 4 µm thick and created with a Physical Vapor

---

* Corresponding author. Tel.: +49 (3494) 6699 - 51265; fax: +49 (3494) 6699 - 54001
E-mail address: m.heimann@q-cells.com

Deposition (PVD) process [1];[7]. In the solar industry, there is no reliable, cost-effective method of directly connecting metallic string ribbons to Al layers [2].

When exposed to oxygen or air, Al instantaneously forms a thin oxide layer that prevents reliable connections with low electrical resistance. *Ultrasonic soldering* is feasible, but requires special solder alloys and has a limited process window. *Standard soldering* is only feasible if another easily solderable layer is applied on top of the Al layer. Long-term stability of the electrical contact resistance of *conductive epoxy joints* to Al surfaces is a concern. All these joining processes require an interconnect material other than string ribbon and rely on a heat-based process. The latter causes heat-induced stress cracks in the silicon, which inhibit progress toward thinner cells.

In the semiconductor industry, however, room temperature ultrasonic bonding of Al ribbons or wires directly to the 3-5μm thick Al top metallization of sensitive power-semiconductor devices is a long-established technology for high-volume, cost-sensitive applications with critical reliability and lifespan requirements, such as under-the-hood automotive electronics [3]. Investigations showed improved reliability of ultrasonically bonded Al ribbons over soldered Cu ribbons for crystalline Si on glass thin-film PV modules [4], and excellent behavior was reported for bussing various CIGS thin-film substrates [5]. Al ribbon costs much less than tin-coated copper (Cu) ribbon even at the larger cross-section needed to compensate for the lower electrical conductivity ($\sigma_{Al} = 3.50 \times 10^7$ S/m, $\sigma_{Cu} = 5.95 \times 10^7$ S/m). The process and materials are well-aligned with the future need for green PV products (RoHS and REACH guidelines) as well as the trend towards thinner cells to significantly reduce material costs.

This study concerns adapting ultrasonic ribbon bonding and equipment used in the semiconductor industry for interconnecting c-Si solar cells to replace soldering.

2. Cell Interconnect

2.1. Process Development

In contrast to soldering or gluing, ultrasonic bonding allows real-time process monitoring and control, as transducer current and frequency, and bond deformation signals can be collected as they happen. These signals, as well as high-speed video observations of bonding sequences, electroluminescence (EL) imaging of bonded cells, bondpeel testing, scanning electron microscopy and optical profiling were used to analyze the process behavior and material characteristics and then correlated to bond results. Due to the great difference in properties between a c-Si cell substrate and a Si power semiconductor mounted to a robust and thick substrate, distinct changes to process and, accordingly, the bond head, workholder, and the ribbon-feed system, had to be developed.

Material analysis, process observations and mechanism analysis showed several effects affecting bond quality and bond yield, especially formation of micro-cracks. Initially c-Si bonding resulted in a yield loss of nearly 100% due to micro-cracking primarily at the bond locations, but identification and elimination of the most significant factors reduced the micro-crack rate to less than 0.2% (36 bonds per cell by over 2000 cells) under well controlled laboratory conditions, with the remaining failures caused by handling errors and cell-metallization flaws. Especially handling problems were more frequent when the equipment processed strings for complete modules in a production environment, resulting in an average micro-crack rate of near 2%.

Process development was performed on mono-crystalline silicon solar cells of typically 160μm thickness, then successfully verified on multi-crystalline cells of similar thickness and mono-crystalline cells as thin as 120 μm. Bondpeel forces greater than 2 N on the *sunny-side* (front) busbars formed from various types of silver (Ag) thick film (thickness about 15 μm) and greater than 5 N on typically 2 μm

thick Al PVD layers on the cell back were achieved without optimizing the bond process. Higher bondpeel forces can be achieved by increasing the bondtool foot area.

2.2. Interconnect Design and Equipment

Creating a reliable ultrasonic bond with low electrical contact resistance requires sufficient relative motion between the ribbon and substrate surface during the initial phase and sufficient strain in the ribbon in the later phase of the bond process. The substrate (thin Si cell) must be firmly held and co-vibration with the bondtool prevented. For the thin, fragile, and flexible c-Si cell, this is achieved by vacuum chucks with special structures specific for bonding on the back and front of the cell. The structures prevent contact between the active cell surface and the workholder and provide needed clamping in the vicinity of the bonds.

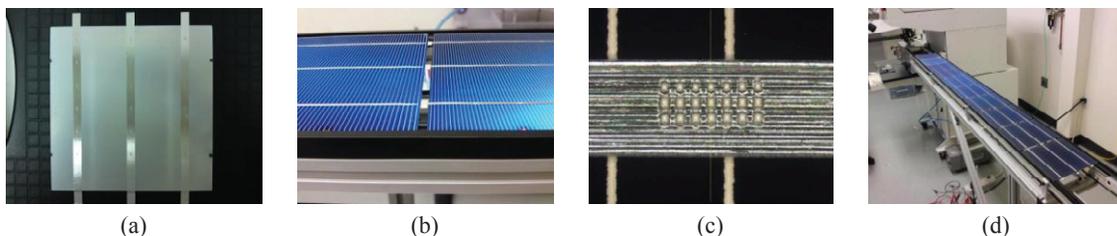| (a) | (b) | (c) | (d) |

Fig. 1. (a) 8mm wide x 0.1 mm thick Al ribbons bonded to the back (7 bonds per ribbon); (b) 2.0 mm (w) x 0.3 mm (t) light-trapping Al ribbons bonded to the fronts of two cells (6 bonds per ribbon/busbar), front-to-back connection between cells; (c) bond on light-trapping ribbon; (d) cell string interconnected on a Kulicke & Soffa 3600 bonder (*stringer*) modified for this application

Standard semiconductor equipment ribbon-feeding and -terminating methods, which allow very accurate and repeatable ribbon placement and termination with very repeatable and short length, were adopted with specific modifications. These modifications enable low micro-crack rates, allow accurately overlapping ribbons with the front busbars to prevent excess or varied shadowing on the active cell area, and connecting front and back ribbons between two cells with a gap of less than 2mm between cells.

The semi-automatic prototype built for this technology evaluation consisted of a first bonder (*tabber*) to tab 8.0 mm (w) x 0.1 mm (t) ribbons of defined lengths to the back of individual cells (Fig. 1 (a)), with one end slightly overhanging the cell edge. Bonding wider, thicker ribbons to the back was successfully tested. On a second bonder (*stringer*), strings were created by bonding 2.0 mm (w) x 0.3 mm (t) light-trapping ribbons on the front busbars of a cell and connecting them to the back ribbons of the next cell (Fig. 1 (b)). While this interconnect concept is serial and needs more handling than current stringers, it offers several advantages. The cross-section, aspect ratio and ribbon type on the front and the back of the cell can be chosen differently and tailored to the needs on the respective side of the cell. Front ribbons should be narrow enough to minimize shadowing the active area but thick enough to minimize the series electrical resistance. Ribbons with a light capturing structure can be used and are as bondable as standard ribbon, see Fig. 1 (c). Back ribbons can be much wider (as there is no shadowing with a large cross-section) than front ribbons to minimize the electrical series resistance.

During the technology assessment, cell handling and string movement had to be done manually, while bonding individual ribbons on front and back of the cells as well as connecting front and back ribbons between two cells was fully automatic at maximum bonder speed. With automated handling, such a line, with standard bonder equipment (serial bonding of busbars) adjusted to the specific process requirements of this application, can process approx. 500 and 700 cells/hour for 3-busbar and 2-busbar cells respectively, with 7 and 6 bonds per back ribbon and front busbar respectively. Higher line productivity will be possible with appropriate equipment development.

3. Analysis on the Solar Cell and Solar Module Level

3.1. Analysis of Shunting the pn-Junction due to Bonding

Shunting of the pn-junction causes a low ohmic connection between the solar-cell basis and emitter. It transforms the diode into a regular resistor and reduces cell performance. A solar-cell emitter is very shallow (approx. 300 nm to 500 nm deep on the *sunny* side). Due to the mechanical nature of the ultrasonic bond process, bonding on the front could therefore induce pn-junction shunting. The result is lower cell performance (depending on the size of the shunt). Because shunts allow large local current flow, they can be detected by cell thermography before and after bonding. Fig. 2 (a) shows such an analysis as example for one cell(more than 20 cells were tested), revealing no detectable shunting from ultrasonic bonding of the ribbons to the front.

3.2. Variation of the Number of Bonds

Ultrasonic bonding creates a finite number of limited-area joints. The objective of this analysis was to determine the minimum number of bonds needed to minimize loss due to the electrical series resistance of the string. Al ribbons were bonded to the front side busbars of fully characterized cells. The number of bonds varied between 1 and 14. In the unbonded areas, tape was placed between the ribbon and busbar to prevent contact. The bonded cells were then again characterized to determine any changes.

In this approach, bond contact resistance is ignored. Effects of the series resistance are related to the distance between bonds and thus depend on the resistance of the Ag busbar on the front or the resistance of the Al layer on the back of the cell. Increased series resistance reduces the Fill Factor (FF), which is directly related to cell performance and is much easier to measure than the series resistance of a diode. Fig. 2 (b) shows that the FF falls significantly for less than 3 bonds/busbar. For cells with 6 or 7 bonds/busbar, as the cells for this study were typically bonded, FF loss is about 1% minimal. This trend, predicted by the theory (red and blue curves), is confirmed by the measurements; however, experimentally determined FF losses are higher than expected, especially for the back.
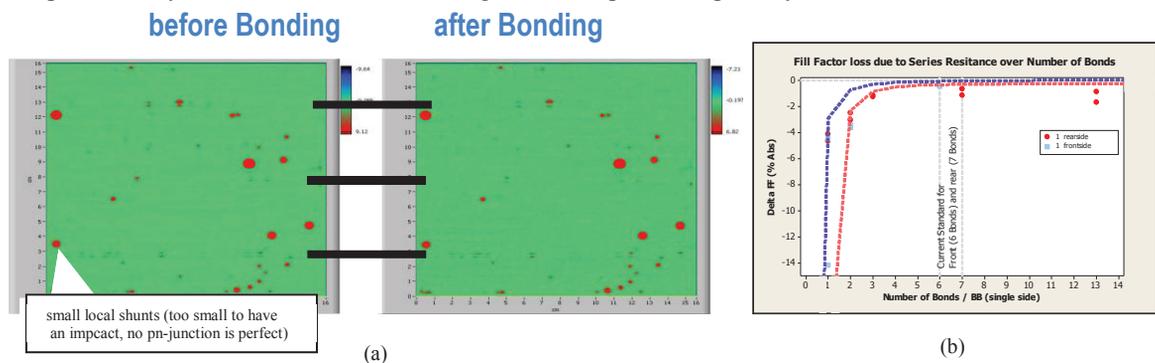

Fig. 2. (a) solar cell thermography pictures showing no difference between before and after bonding ribbons to the front of the cell; (b) fill factor loss simulation (curves) and actual measurement data as a function of the number of bonds

3.3. Module Assembly and Climate Chamber Tests

The aim of this investigation was to develop Al ribbon bonding to interconnect c-Si solar cells in modules replacing standard soldering technology. On the *sunny* side, Al ribbons are bonded to the Ag busbar and on the back to a thin Al layer.
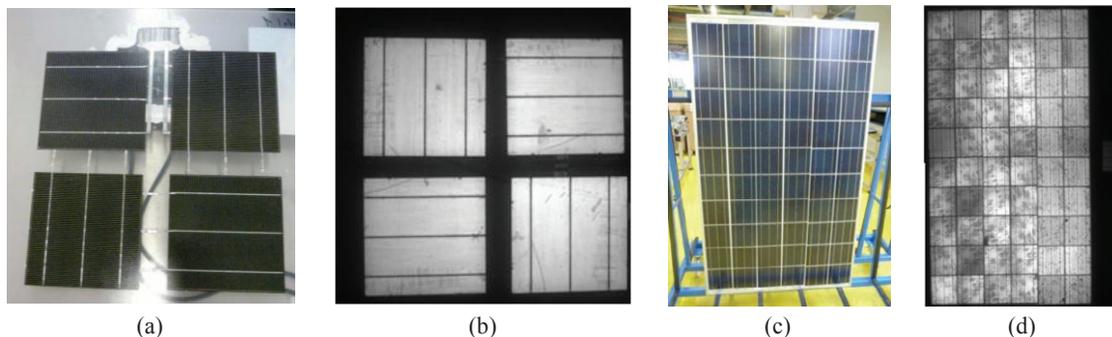
Fig. 3. (a) Mini-module; (b) EL image of mini-module; (c) finished 60-cells-module; (d) EL image of 60-cells-module

In a first step, c-Si cells with Al ribbons bonded to the screen-printed Ag thick-film busbars on the front and to the Al PVD layer on the back of c-Si cells without micro-cracking were successfully tested. The cells exhibited good bondpeel strength and no micro-cracking after thermal cycling, and good electrical contact quality after damp heat testing. In a second step, mini-modules (2 x 2 cells per module, Fig. 2 a) manually strung with soldered cross-connections, were assembled and successfully tested (thermal cycling, damp heat, humidity freeze) in the climate chamber. In a third step, many cells were bonded and assembled into standard-size, 60-cells-modules (Fig. 2 c). At a maximum acceptable micro-crack rate of 5%, modules were built without major cracking problems (micro cracking rate lower than 2%).

Table 1. Changes in electrical parameters for an ultrasonically bonded 60-cell module after various climate-chamber tests (excerpt)

Damp heat 1000 h	ΔImpp	ΔUmpp	ΔFF	ΔPmpp
500 h	−0,17%	−0,05%	−0,15%	−0,20%
1,000 h	−0,44%	−0,59%	−1,80%	−1,63%
Thermal cycling (t. c.) 50 cycles + 10 cycles humidity freeze (h. f.)	ΔImpp	ΔUmpp	ΔFF	ΔPmpp
50 cycles t.c.	-0,22%	-0,04%	-0,15%	-0,10%
10 cycles h.f.	-1,32%	-0,89%	-1,63%	-2,35%
Thermal cycling 200 cycles	ΔImpp	ΔUmpp	ΔFF	ΔPmpp
100 cycles	-0,37%	-0,07%	-0,25%	-0,30%
200 cycles	-4,14%	-1,59%	-2,88%	-5,66%

With automated cell handling, well-trained and experienced operators should have no more difficulty assembling modules with cells interconnected by bonding compared to the present solder process. Six modules with six ultrasonically interconnected strings of 10 cells each were assembled with hand-soldered cross-connections between strings. The modules were tested according to IEC61215. The modules are conventionally packaged assemblies of solar glass, polymer foil, ultrasonically tabbed and stringed cells, cross-connected with hand soldering, polymer foil, and a transparent back-sheet. The IEC test consists of several climate-chamber tests: damp heat, thermal cycle, and humidity freeze. The criterion for test failure is a power loss of more than 5 % [6].

The power loss for these modules, shown in Table 1, is less than 5% after 1,000 hours of damp-heat testing and 50 temperature cycles combined with 10 humidity-freeze cycles. Only for thermal cycling did the power loss fall below the criterion; consequently, more investigations due to contact resistance versus climate-chamber testing of the bonds were done.
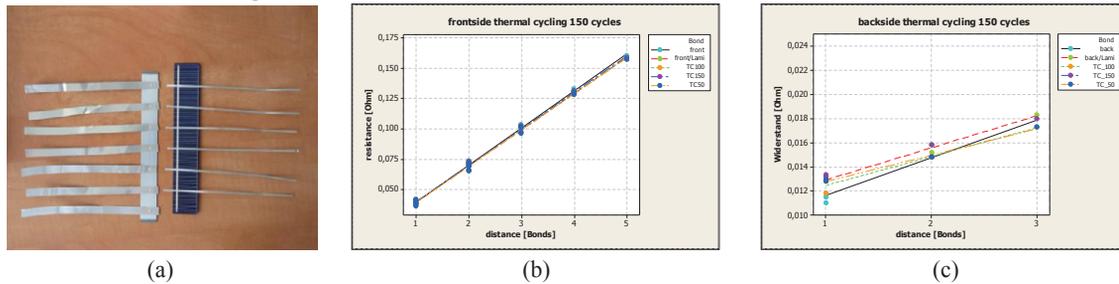

Fig. 4. (a) TLM structure; (b) contact resistance measurement front (thermal cycling test) (c) contact resistance measurement back (thermal cycling test)

A main observation was the severe degradation of the hand-soldered cross-connections. To independently determine the behavior of the bonded joints on the cells, Transmission Line Method (TLM) structures for the front and back were created and tested separately (Fig. 4). As a result, it is concluded that there is no contribution from the bonds on the cells to a change in module performance during the climate-chamber tests. Ultrasonic bonding of the cross-connections is quite feasible as demonstrated with the front-to-back ribbon connection between two cells in a string as shown in Fig. 1 (b). Another bonder would be needed, which, in volume production could be shared by several *tabber-stringer* lines.

4. Conclusions

Feasibility to tab and string crystalline silicon solar cells with room-temperature ultrasonic bonding of Al ribbons was demonstrated. The data show that the process is robust, allows reducing cost (by using Al instead of Cu), and eliminating Ag pads, and creating a comparable reliability for both the Al ribbon-to-Al PVD layer interface on the back of the cell and the Al ribbon-to-Ag thick-film interface on the front of the cell to standard soldered modules. The prototype equipment used for the study could be automated to fulfil production throughput requirements.

References

[1] R. Hezel and K. Jaeger, J. Electrochem. Soc.1989; 136, 518

[2] Nekarda J-F, Hoerteis M, Lottspeich F, Wolf A, Preu R, Comparison of three different metallization concepts for LFC cells. Proceedings of the 25th European PVSEC, 2010.

[3] Liang, Z, Power Device Packaging, U.S. Department of Energy, ORNL/TM-2010/204; 2010, p.90-100.

[4] Jarnasson S, Luechinger C, Accelerated Testing of Ultrasonic Welding for Crystalline Silicon on Glass Modules. Proceedings of the 23rd European PVSEC, 2008.

[5] Xu T, Valentin O, Luechinger C, Reliable metallic tape connection on CIGS solar cells by ultrasonic bonding. In: Delahoy AE, Eldada LA, editors. Thin Film Solar Technology II, SPIE Proceedings Vol. 7771, 2010.

[6] Mohr A. et al, 20%-efficient rear side passivated solar cells in pilot series designed for conventional module assembling. Proceedings of the 26rd European PVSEC, 2011.

[7] R. Hezel, Advances in MIS inversion layer solar cells, in IEEE Photovoltaic Specialists Conference (IEEE, Las Vegas, 1985), pp. 180-185.